Available online at www.sciencedirect.com
ScienceDirect
Ceramics International 37 (2011) 2723–2726
CERAMICS INTERNATIONAL
www.elsevier.com/locate/ceramint

Co-doping effect of Zn and Sb in SnO_2: Valence stabilization of Sb and expanded solubility limit

Dong-Kyun Kim [a], Joon-Hyung Lee [a], Young-Woo Heo [a], Hee Young Lee [b], Jeong-Joo Kim [a,*]

[a] School of Materials Science and Engineering, Kyungpook National University, Daegu 702-701, Republic of Korea
[b] School of Materials Science and Engineering, Yeungnam University, Gyeongsan 712-749, Republic of Korea

Received 8 February 2011; received in revised form 12 April 2011; accepted 13 April 2011
Available online 21 April 2011

Abstract

In this study, the co-doping effect of ZnO and Sb_2O_5 on the solubility limit in SnO_2 was investigated. When ZnO was added to SnO_2, its solubility limit was around 3 at%, while that of Sb_2O_5 could not be evaluated due to the severe evaporation of Sb_2O_5 during sintering. For the co-doping of ZnO and Sb_2O_5, the $ZnSb_2O_6$ phase was used for the source of Zn and Sb dopants to prevent the evaporation of Sb_2O_5. When ZnO and Sb_2O_5 were co-doped by $ZnSb_2O_6$, the solubility limit expanded to 60 at%. XPS analysis of the Sb revealed that Sb^{5+} is stable when Zn is co-doped. The extended solubility limit is explained by electrostatic and strain energy minimization in the lattice.

Keywords: SnO_2; Co-doping; Solubility limit; Charge compensation; XPS

1. Introduction

SnO_2 ceramic is, intrinsically, an n-type semiconductor due to the oxygen deficiencies and has a high energy band gap greater than 3.54 eV. Because of its low resistivity of 10^{-3} Ω cm and high transmittance of over 80% in the visible region, SnO_2 is applicable for transparent conducting oxide (TCO) and has been widely used as a transparent heating element, gas-detecting sensor and electrode for electric glass-melting furnaces [1–3].

For the exploitation and tailoring of useful TCO materials, the substitution or doping of cation is one of the most promising methods which can lead to improved optical and electrical properties, modified band gap energy, and others. In the case of In_2O_3, for making Sn-doped In_2O_3 (indium tin oxide), the solubility limit of SnO_2 in In_2O_3 is about 6–8 at% [4]. While the solubility limit of Zn^{2+} in In_2O_3 is close to 1 at% [5]. These results suggest that the respective solubility limits of Sn^{4+} and Zn^{2+} in In_2O_3 are relatively low. However, when Sn^{4+} and Zn^{2+} are co-doped in In_2O_3, an enormous solid solution of Sn^{4+} and Zn^{2+} was reported [6–8].

When both Sn^{4+} and Zn^{2+} are substituted with the 1:1 ratio in In_2O_3, the total amount of soluble Sn^{4+} and Zn^{2+} can be expanded up to 40 at%. The reason for this is due to the charge compensation between Sn^{4+} and Zn^{2+} since Sn and Zn ions have an opposite effective charge with respect to In ions and a charge compensation can be obtained without any defect formation [6–8]. Similarly, when Zn^{2+} was added to 20 at% Sn^{4+} contained In_2O_3, in which a large amount of $In_4Sn_3O_{12}$ second phase is presented, the amount of the second phase decreased as the content of Zn^{2+} increased [9].

The energy necessary in such cases is lower than a case in which there is a charge compensation through defect formation. Consequently, the solubility limit can be extended when two dopants, which have opposite effective charges, are added to a matrix by their mutual effect, when compared with the solubility limit of the addition of a single dopant [9].

The current study examined the co-doping effects of Sb^{5+} and Zn^{2+} in SnO_2. The solubility limits of the single dopant Sb_2O_5 and ZnO were examined. Then Sb and Zn co-doping was carried out. In the case of the simultaneous substitution of Sb^{5+} and Zn^{2+} for Sn^{4+} in SnO_2, the charge compensation should be considered. So, the $ZnSb_2O_6$ phase, which is composed of Zn and Sb with an atomic ratio of 1:2, was synthesized and added to SnO_2. Since Sb has various valence states and it can affect the charge compensation in co-doped SnO_2, an XPS study was

* Corresponding author. Tel.: +82 53 950 5635; fax: +82 53 950 5645.
E-mail address: jjkim@knu.ac.kr (J.-J. Kim).

0272-8842/$36.00
doi:10.1016/j.ceramint.2011.04.026

conducted. The extended solubility limit by co-doping was discussed on the basis of electrostatic and strain energy minimization.

2. Experimental procedure

SnO_2 (Aldrich Chemical Co., USA, 99.9%), ZnO (Sigma Aldrich, 99.9%, USA) and Sb_2O_5 (high purity chemicals, 99.9%, Japan) were used as the starting chemicals for the general solid-state reaction method of oxides. Since Sb_2O_5 melts at the relatively low temperature of 525 °C and easily evaporates during the reaction and/or sintering at high temperature [10], the dopants of Sb_2O_5 and ZnO were not added directly to the SnO_2. Instead, the $ZnSb_2O_6$ phase, in which Zn and Sb cations are composed of a ratio of 1:2, was synthesized by a solid state reaction route at 600 °C for 2 h. The amount of $ZnSb_2O_6$ to SnO_2 was varied with Sn:$ZnSb_2$ ratios of 90:10, 70:30, 50:50, 30:70 and 10:90, i.e., the x value in the $Sn_{1-x}Zn_{x/3}Sb_{2x/3}O_2$ system was changed so that $x = 0.1$, 0.3, 0.5, 0.7 and 0.9.

The weighed raw powders were wet-ball milled with ethyl alcohol for 24 h. After drying, the powder was formed into pellets by a sequential process of weak uniaxial pressing, followed by cold isostatic pressing (CIP) at 250 MPa. Sintering was conducted at 1300 °C for 2 h in a pure oxygen ambient (O_2; 99.9%) with a heating rate of 5 °C/min.

The weight loss of the samples during sintering was measured using a DTA/TG (320 & SSC 5200H Disk Station, Seiko, Japan). The microstructure of the specimen surfaces was observed by using a scanning electron microscope (Hitachi, S-4300&EDX-350, Tokyo, Japan). X-ray diffraction with nickel-filtered Cu-Kα radiation (Mac Science, M03XHF, Yokohama, Japan) and energy dispersive X-ray analysis (EDXA; Oxford, Model 6587, High Wycombe, UK) were used for phase identification. XPS (ESCALAB 250 XPS spectrometer, VG Scientifics, UK) studies were also conducted to analyze the chemical shift of Antimony in the sintered samples in the range of 550–520 eV at 0.2 eV intervals.

3. Results and discussion

In order to determine the respective solubility of Sb_2O_5 and ZnO in SnO_2, even though detailed experimental results are not presented, various amounts of the dopants were solely doped in SnO_2 and sintered at 1300 °C for 2 h in oxygen. The powder X-ray diffraction of the sintered samples revealed that, in the case of the Sb_2O_5 doping, no diffraction peaks from the second phases were observed and the SnO_2 single phase was maintained even though the amount of Sb_2O_5 was increased up to 35 at%. On the basis of the weight loss monitored by a DTA/TG, 98–99% of the Sb_2O_5 evaporated during sintering and it resulted in porous microstructures. The amount of residual Sb in the samples with 10, 20, 30 and 35 at% Sb doped SnO_2 was analyzed by an EDS, and only 0.47, 0.94, 1.20 and 2.40 at% of Sb was found, respectively. In the case of ZnO doping, however, a second phase of Zn_2SnO_4 (JCPDS no. 24-1470) appeared in the X-ray diffraction when 3 at% of ZnO was doped. Therefore, it is thought that the respective solubility of Sb_2O_5 and ZnO in SnO_2 is quite small.

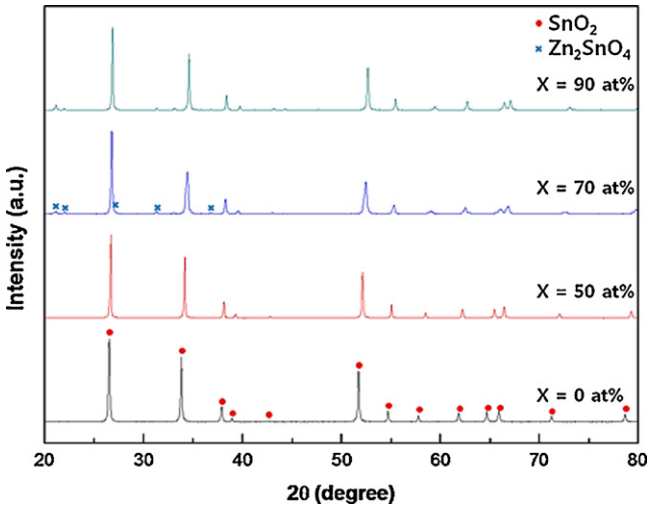

Fig. 1. X-ray diffraction patterns of $Sn_{1-x}Zn_{x/3}Sb_{2x/3}O_2$ system. Samples were sintered at 1300 °C for 2 h in O_2.

On the other hand, the solubility increased greatly when Zn and Sb were co-doped at a 1:2 ratio. Fig. 1 shows the X-ray diffraction patterns of the $Sn_{1-x}Zn_{x/3}Sb_{2x/3}O_2$ samples as a function of x which was sintered at 1300 °C for 2 h in oxygen. The single phase of SnO_2 was maintained until $x = 0.6$ while a small amount of the second phase of the Zn_2SnO_4 appeared when $x = 0.7$. However, it is not reasonable to determine the solubility limit as simply being $x = 0.7$ when the severe evaporation of Sb is concerned which was previously observed. Table 1 summarizes the cationic compositions of the sintered samples obtained by an EDS analysis. The results yield a tendency that the more $ZnSb_2O_6$ dopants, the more the Sb deficiency. The weight loss of the samples after sintering as a function of x is presented in Fig. 2. The maximum weight loss

Table 1
A summary of cationic ratios by EDS analysis in sintered $Sn_{1-x}Zn_{x/3}Sb_{2x/3}O_2$ samples.

Element	x				
	$x = 0.1$ Zn: 3.33 at% Sb: 6.67 at%	$x = 0.3$ Zn: 10 at% Sb: 20 at%	$x = 0.5$ Zn: 16.7 at% Sb: 33.3 at%	$x = 0.7$ Zn: 23.3 at% Sb: 46.7 at%	$x = 0.9$ Zn: 30 at% Sb: 60 at%
Sn L	89.17	69.43	49.29	28.80	9.42
Zn K	4.22	10.95	17.80	29.04	33.65
Sb L	6.61	19.62	32.91	42.15	56.93
Total	100	100	100	99.99	100

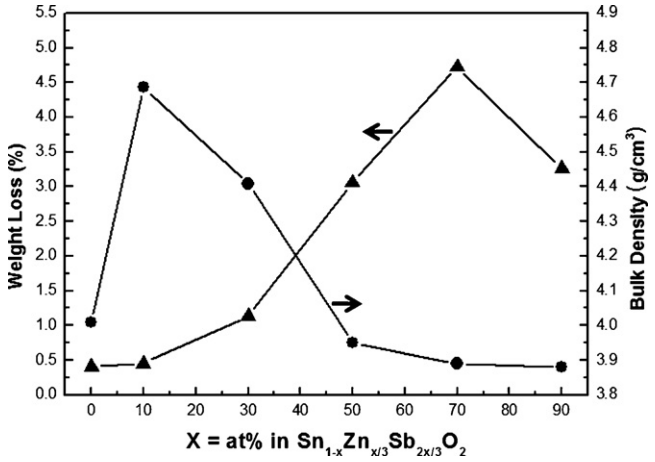

Fig. 2. Weight loss (▲) and bulk density (●) of $Sn_{1-x}Zn_{x/3}Sb_{2x/3}O_2$ samples.

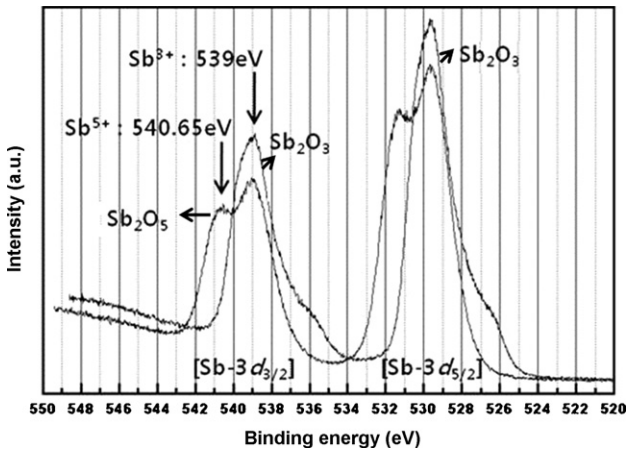

Fig. 4. XPS narrow scan of antimony oxides for a reference.

reached around 4.7% when $x = 0.7$. Therefore, it is presumed that the development of the Zn_2SnO_4 second phase at $x = 0.7$ is partly attributed to the Sb evaporation, which induced a charge unbalance between the Zn^{2+} and Sb^{5+} in SnO_2. Note that the amount of Sb evaporation decreased greatly in the $ZnSb_2O_6$ doped samples when compared with the samples doped solely with Sb_2O_5.

Fig. 3 shows the lattice constants of the sintered samples. The solid lines are the lattice constants of the samples calculated and modified on the basis of X-ray diffraction and cationic composition. For a comparison, the lattice constants of SnO_2 and $ZnSb_2O_6$ are marked and connected with dotted lines to see if the experimental results agree well with Vegard's law.

In order to investigate the valence state of Sb in the sintered samples, an XPS analysis for the raw chemicals of Sb_2O_5 and Sb_2O_3 (both are the products of the same company) was conducted, and the results are shown in Fig. 4 as a reference. The analysis for Sb_2O_3 revealed that the peaks of $3d_{3/2}$ and $3d_{5/2}$ appeared at 539.00 eV and 529.65 eV, respectively, which is in agreement with the results found in previous studies [11]. However, Sb_2O_5 presents a simultaneous existence of Sb_2O_5 and Sb_2O_3, showing not only $3d_{3/2}$ and $3d_{5/2}$ peaks at 540.65 eV and 531.30 eV, respectively from Sb_2O_5 but also $3d_{3/2}$ and $3d_{5/2}$ peaks at 529.65 eV and 539.00 eV, respectively from Sb_2O_3 [11]. Because Sb_2O_5 is known to have a metastable phase at atmospheric pressure [12], both Sb_2O_5 and Sb_2O_3 exist together as shown in Fig. 4.

Fig. 5 shows the XPS spectra of the sintered samples as a function of the dopants Sb_2O_5 and ZnO in $Sn_{1-x}Zn_{x/3}Sb_{2x/3}O_2$ where $x = 0.1$, 0.3 and 0.5. The results revealed that the peaks for Sb-$3d_{3/2}$ and $3d_{5/2}$ are composed of Sb^{5+} only at 540.50 eV and 531.00 eV, respectively, regardless of the amount of dopants and no traces of Sb^{3+} were found. The small discrepancy in the peak position less than 0.3 eV between the reference (Fig. 4) and the samples (Fig. 5) is caused by the chemical shift of Sb (binding energy difference in Sb_2O_5/Sb_2O_3 and $Sn_{1-x}Zn_{x/3}Sb_{2x/3}O_2$).

In the Sn–Sb binary oxide systems, it is reported that the concentration of Sb^{3+} and Sb^{5+} is competitive when the antimony doping level or annealing temperatures are changed. According to Terrier et al. [13], antimony exists under two oxidation states of Sb^{5+} and Sb^{3+} in doped SnO_2 films, and the Sb^{3+} component overcomes the Sb^{5+} component as the doping level increases. Rockenberger et al. [14] and Jayakumar et al. [15] reported that an annealing temperature dependence of the

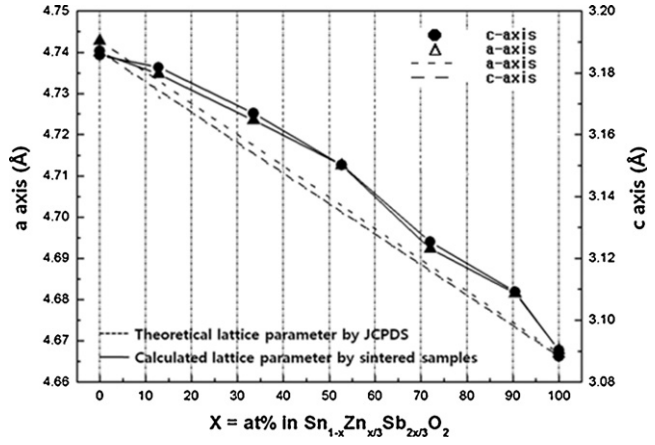

Fig. 3. Lattice constants of *a*-axis (▲) and *c*-axis (●) of $Sn_{1-x}Zn_{x/3}Sb_{2x/3}O_2$ samples. Dot lines exhibit theoretical lattice constants evaluated from the values in the JCPDS and solid lines exhibits lattice constants of sintered samples evaluated from the X-ray diffraction.

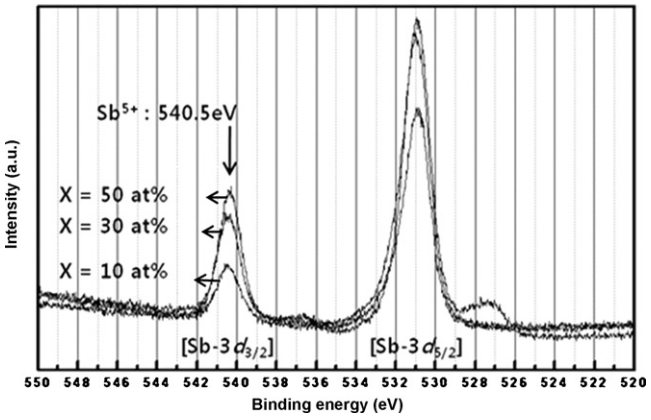

Fig. 5. XPS narrow scan of $Sn_{1-x}Zn_{x/3}Sb_{2x/3}O_2$.

valence state that the concentration of Sb^{3+} is predominant over 500 °C. These results were explained by a thermodynamic reason whether the valence of Sb is in a stable or metastable atmospheric state [12].

Unlikely to the previous results, we observed only Sb^{5+} in the samples in which the charge compensation was satisfied when Zn and Sb are co-doped at the 1:2 ratio. This can be expressed by

$$ZnO + Sb_2O_5 \underset{3SnO_2}{\longrightarrow} Zn''_{Sn} + 2Sb^{\bullet}_{Sn} + 6O^{x}_{O}$$

In this case, the complete charge compensation is maintained without defect generation and the electrostatic energy can be minimized. On the other hand, concerning the doping induced stain energy in the lattice, since the ionic radius of Zn^{2+} (0.074 nm) is larger and Sb^{5+} (0.06 nm) is smaller than Sn^{4+} (0.069 nm), the strain energy of the lattice will be decreased by the co-doping of Zn^{2+} and Sb^{5+}. Consequently, from the electrostatic and mechanical energy viewpoint, it is understood that the electrical charge and stain energy compensation by the co-doping extended the solubility limit up to $x = 0.6$ in $Sn_{1-x}Zn_{x/3}Sb_{2x/3}O_2$.

4. Conclusion

When Sb_2O_5 and ZnO were added to SnO_2, their respective solubility limits were small. However, when $ZnSb_2O_6$, which is composed of Zn and Sb with an atomic ratio of 1:2, was doped in SnO_2, the solubility limit increased greatly to 60 at%. In this case, the electrostatic energy can be minimized by the charge compensation when Zn and Sb are co-doped with an atomic ratio of 1:2. The XPS analysis of Sb supports the charge compensation between Zn^{2+} and Sb^{5+} which showed only Sb^{5+} in the sample. Furthermore, the strain energy of the lattice can be reduced when Zn^{2+} (0.074 nm) and Sb^{5+} (0.06 nm) are simultaneously substituted for Sn^{4+} (0.069 nm). The extended solubility limit by co-doping was explained by the total energy reduction.

Acknowledgements

This work was supported by the Priority Research Centers Program, the Mid-career Researcher Program, and the Basic Science Research Program through the National Research Foundation of Korea (NRF) grant funded by the Korean government (MEST) (nos. 2009-0093819, 2007-0056848, 2010-0001871, and 2010-0001874).

References

[1] J.G. Fagan, V.R.W. Amarakoon, Am. Ceram. Bull. 72 (3) (1993) 119.
[2] G. Williams, G.S.V. Coles, The gas-sensing potential of nanocrystalline tin dioxide produced by a laser ablation technique, MRS Bull. 24 (6) (1999) 25–29.
[3] R.G. Gordon, Criteria for choosing transparent conductors, MRS Bull. 25 (8) (2000) 52–57.
[4] G. Frank, H. Kostlin, Electrical properties and defect model of tin-doped indium oxide layers, Appl. Phys. A: Solids Surf. 27 (4) (1982) 197–206.
[5] D.H. Park, K.Y. Son, J.H. Lee, J.J. Kim, J.S. Lee, Effect of ZnO addition in In_2O_3 ceramics: defect chemistry and sintering behavior, Solid State Ionics 172 (1–4) (2004) 431–434.
[6] G.B. Palmer, K.R. Poeppelmeier, T.O. Mason, Conductivity transparency of ZnO/SnO_2-cosubstituted In_2O_3, Chem. Mater. 9 (12) (1997) 3121–3126.
[7] A. Ambrosini, G.B. Palmer, A. Maignan, K.R. Poeppelmeier, M.A. Lane, P. Brazis, C.R. Kannewurf, T. Hogan, T.O. Mason, Variable-temperature electrical measurements of zinc oxide/tin oxide-cosubstituted indium oxide, Chem. Mater. 14 (1) (2002) 52–57.
[8] A. Ambrosini, S. Malo, K.R. Poeppelmeier, M.A. Lane, C.R. Kannewurf, T.O. Mason, Zinc doping in cosubstituted $In_{2-2x}Sn_xZn_xO_{3-\delta}$, Chem. Mater. 14 (1) (2002) 58–63.
[9] K.H. Seo, D.H. Park, J.H. Lee, J.J. Kim, Co-doping effect of SnO_2 and ZnO in In_2O_3 ceramics: change in solubility limit and electrical properties, Solid State Ionics 177 (5–6) (2006) 601–605.
[10] G.V. Samsonov, The Oxide Handbook, IFI/Plenum, New York, 1982.
[11] C.D. Wagner, W.M. Riggs, L.E. Davis, J.F. Moulder, in: G.E. Muilenberg (Ed.), Handbook of X-ray Photoelectron Spectroscopy, Perkin Elmer Co., Minnesota, 1979, pp. 120–121.
[12] N.A. Asryan, A.S. Alikhanyan, G.D. Nipan, Specifics of sublimation of antimony oxides, Phys. Chem. 392 (2003) 221–226.
[13] C. Terrier, J.P. Chatelon, J.A. Roger, Analysis of antimony doping in tin oxide thin films obtained by the sol–gel method, J. Sol–Gel. Sci. Technol. 10 (1997) 75–81.
[14] J. Rockenberger, U. Zum Felde, M. Tischer, L. Troger, M. Haase, H. Weller, Near edge X-ray absorption fine structure measurements (XANES) and extended X-ray absorption fine structure measurements (EXAFS) of the valence state and coordination of antimony in doped nanocrystalline SnO_2, J. Chem. Phys. 112 (9) (2000) 4296–4304.
[15] O.D. Jayakumar, V. Sudarsan, S.K. Kulshreshtha, Metallic nature of $Sn_{1-x}Sb_xO_{2\pm\delta}$ ($x = 0.0$ 0. 10, and 0. 20) mixed oxides: probed by ^{119}Sn MAS NMR, Phys. B 392 (2007) 67–71.